NUCLEAR BURNING

- CHAINS, CYCLES & PROCESSES

- HYDROSTATIC BURNING
  - GENERATE ENERGY to oppose GRAVITY
  - NUCLEOSYNTHESIS : DIRECT & INDIRECT
- EXPLOSIVE BURNING / NUCLEOSYNTHESIS
  - GRAVITY HAS LOST THE FIGHT OR IS NOT IN CONTROL

HYDROSTATIC BURNING

- FUEL SEQUENCE

$$H \Rightarrow He \Rightarrow C \Rightarrow Ne \Rightarrow O \Rightarrow Si$$
$$*$$

- NUCLEAR COMPLEXITY INCREASES $H \Rightarrow Si$ AS $T \uparrow$
- OPPORTUNITIES FOR DIRECT & INDIRECT N' SYNTHESIS INCREASES down the sequence
- ENERGY LOSS TO NEUTRINOS INCREASES DOWN THE SEQ.

$$2\delta \rightarrow e^+ + e^- \Rightarrow \nu_e + \bar{\nu}_e$$

H-burning

- EDDINGTON

  $4 m_H > m_{He}$ by 0.7%

  $E = \Delta m c^2$

- BETHE (1939)

  CN-cycle convert 4H ⇒ He with C & N as CATALYSTS

- **STELLAR AGES**

$$\tau_{Nuc}(H) \sim \frac{\epsilon f M c^2}{L}$$

For $L \propto m^4$ (main-seq.)

$$\tau_{Nuc}(H) \sim \frac{\epsilon f}{(m/M_\odot)^3} \frac{M_\odot c^2}{L_\odot}$$

$$\sim 3 \times 10^{10} \left(\frac{M_\odot}{m}\right)^3 \text{ yrs}$$

for $\epsilon = 0.0071$ and $f \sim 0.3$

H-burning

- The pp-chains
- The CNO cycles

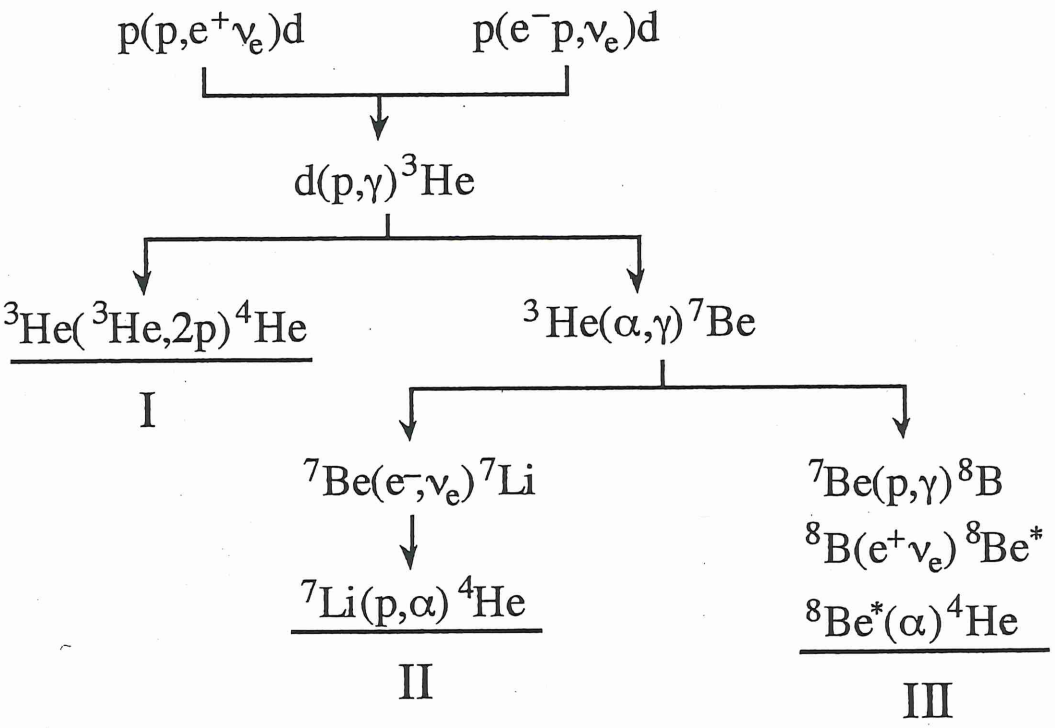

Fig. 3.1. The *pp*-chains that convert hydrogen to helium.

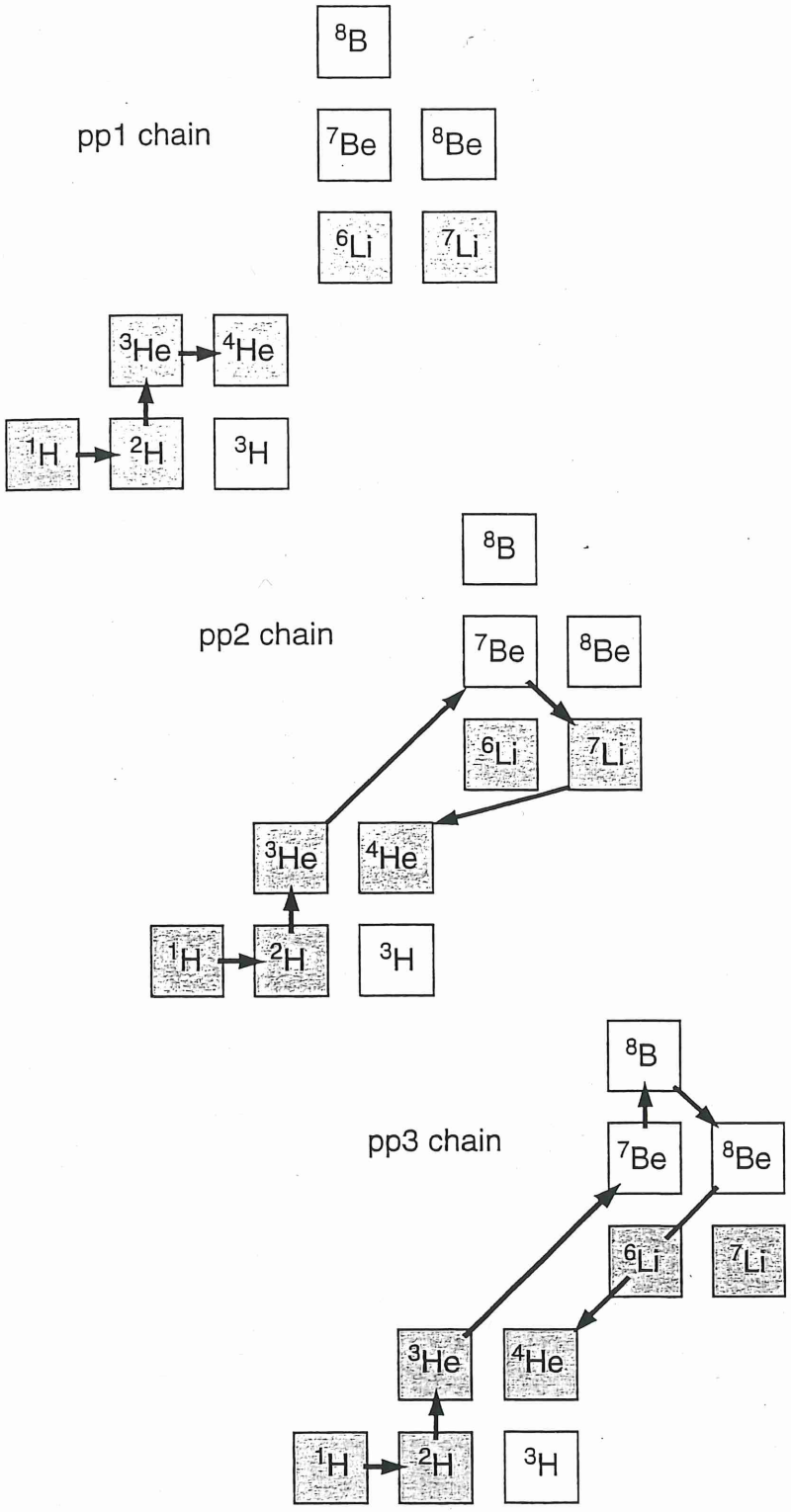

Figure 5.2 Representation of the pp chains in the chart of the nuclides. Each arrow represents a specific nuclear interaction connecting the initial with the final nucleus. For example, the reaction $^3He(\alpha,\gamma)^7Be$ is represented by an arrow extending from ^3He to ^7Be (middle and bottom panel). Each of the pp chains effectively fuses four protons to one ^4He nucleus. Stable nuclides are shown as shaded squares.

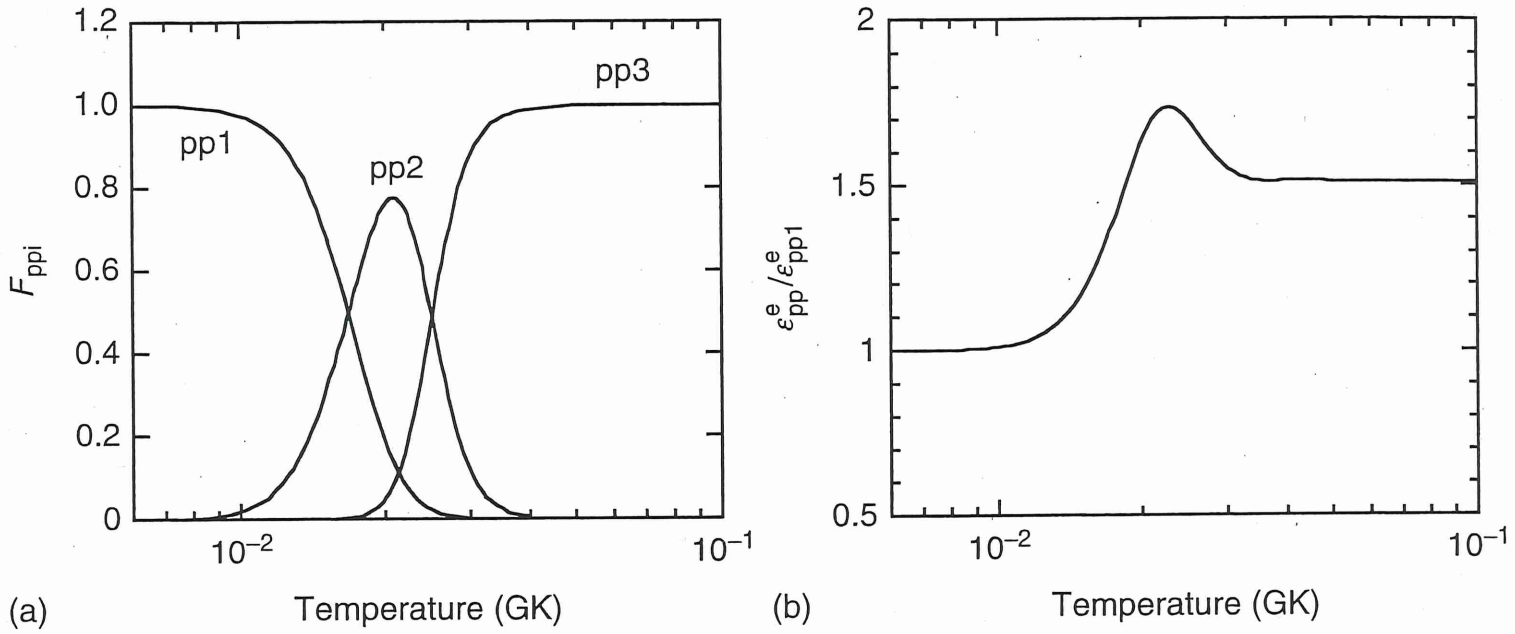

Figure 5.7 (a) Fraction of ^{4}He nuclei produced by the pp1, pp2, and pp3 chains, which are the main producers of ^{4}He at temperatures of $T < 18$ MK, $T = 18$–25 MK, and $T > 25$ MK, respectively. (b) Ratio of the energy generation rate by all three pp chains to that by the pp1 chain alone versus temperature. The ratio is unity for $T < 10$ MK, where the pp1 chain dominates. The maximum at $T \approx 23$ MK is caused by the dominant operation of the pp2 chain. About 90% of the Sun's energy is produced by the pp1 chain. All curves shown are independent of density and are calculated for a composition of $X_H = X_\alpha = 0.5$ and a fully ionized gas.

THE pp-CHAINS

CONTROLLING REACTION

$$p + p \rightarrow {}^{2}H + e^{+} + \nu_e$$

= WEAK INTER.

- NOT MEASURABLE [$\sigma \sim 10^{-23}$ b at 1 MeV
- CALCULATED

NUCLEOSYNTHESIS

- DIRECT: ^{2}H DESTROYED
  ^{3}He ↑ IN LOW MASS ⋆
  ^{4}He !
- INDIRECT: Li, Be, B ↓

SOLAR ν's ^{8}B ν's → SOLAR NEUTRINO PROBLEM

PROTON LIFETIMES

set by $p+p$ REACTION

$$\frac{dn_p}{dt} = -n_p^2 \langle \sigma v \rangle_{pp}$$

$$\tau_p = \frac{1}{\frac{1}{n_p}\frac{dn_p}{dt}} = \frac{1}{n_p \langle \sigma v \rangle_{pp}}$$

Assume $\rho = 100$ g/cm^3 , $X_H = 1$

↘ 100 moles/cm^3

Rate from NACRE

T_6 (K)	5	10	20	30	40
τ_p (Gyr)	880	23	1.4	0.33	0.15

DEUTERIUM ABUNDANCE ?

$p + p \rightarrow d + e^+ + \nu_e$: V. SLOW

$d + p \Rightarrow {}^3He + \gamma$: FAST

$$\left(\frac{D}{H}\right)_{eq} = \frac{\langle \sigma v \rangle_{pp}}{2\langle \sigma v \rangle_{pd}}$$

T_6 (K)	5	10	15
$(D/H)_{eq}$	7.5,-18	4.8,-18	3.9-18

RATES from NACRE

$(D/H)_{eq} \ll (D/H)_{Big\ Bang}$

D is ASTRATED

TIME to EQUILIBRIUM

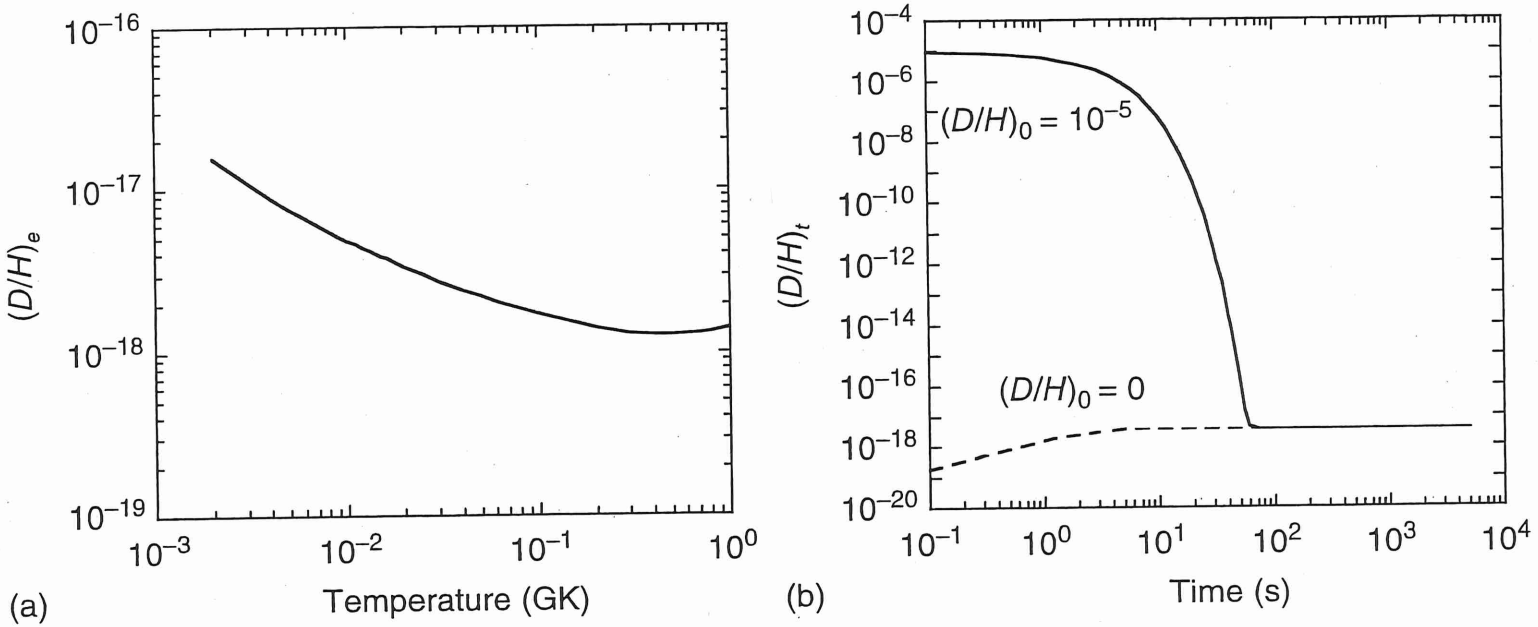

Figure 5.3 (a) Equilibrium abundance ratio $(D/H)_e$ versus stellar temperature. (b) Time evolution of the abundance ratio (D/H) for the conditions $T = 15$ MK, $\rho = 100$ g/cm^3, and $X_H = 0.5$. The dashed and solid lines are obtained for initial deuterium abundances of $(D/H)_0 = 0$ and $(D/H)_0 = 10^{-5}$, respectively. In either case, the deuterium abundance reaches equilibrium in a time negligible compared to the lifetime of stars.

^{3}He PRODUCTION?

- CORES OF LOW MASS MS STARS can be net producers of ^{3}He
  - FACTOR IN CORRECTING ^{3}He spin-flip OBS. FOR BIG BANG ^{3}He/H
  - LATER, ^{7}Li; PRODUCTION VIA CAMERON-FOWLER MECHANISM

Assume pp I dominant

$$\frac{dn_3}{dt} = n_p n_d \langle \sigma v \rangle_{pd} - n_3^2 \langle \sigma v \rangle_{33}$$

$$= 0 \quad \text{in equilibrium}$$

$$\left(\frac{^3He}{H}\right)_{eq} = \left[\frac{\langle \sigma v \rangle_{pp}}{2 \langle \sigma v \rangle_{33}}\right]^{1/2}$$

T_6	10	20	30	40
$(^3He/H)_{eq}$	1.8-4	2.7-6	3.3-7	9.2-8

——— ASTRATED

——— SYTHESIZED ———

← TIME TO EQ. V. LONG

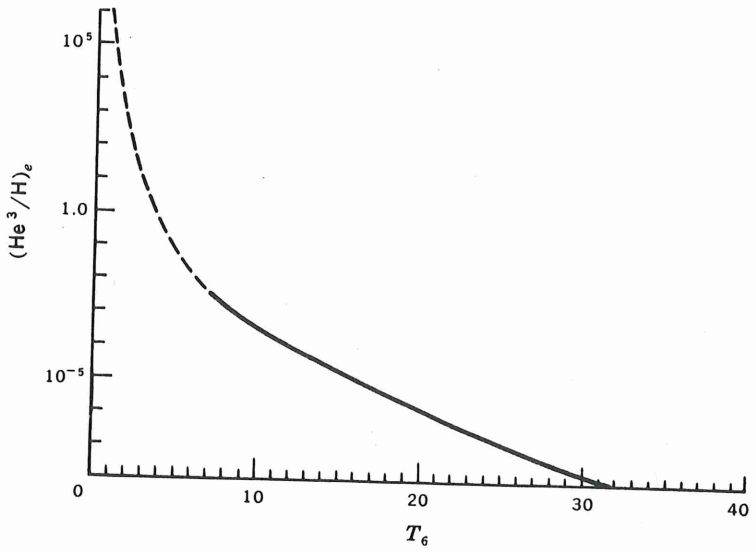

Fig. 5-4 The equilibrium concentration of He^3 during hydrogen burning. The curve is dashed for $T_6 < 8$ because the length of time required for He^3 to achieve equilibrium at such low temperatures is unreasonably long.

From Clayton's book

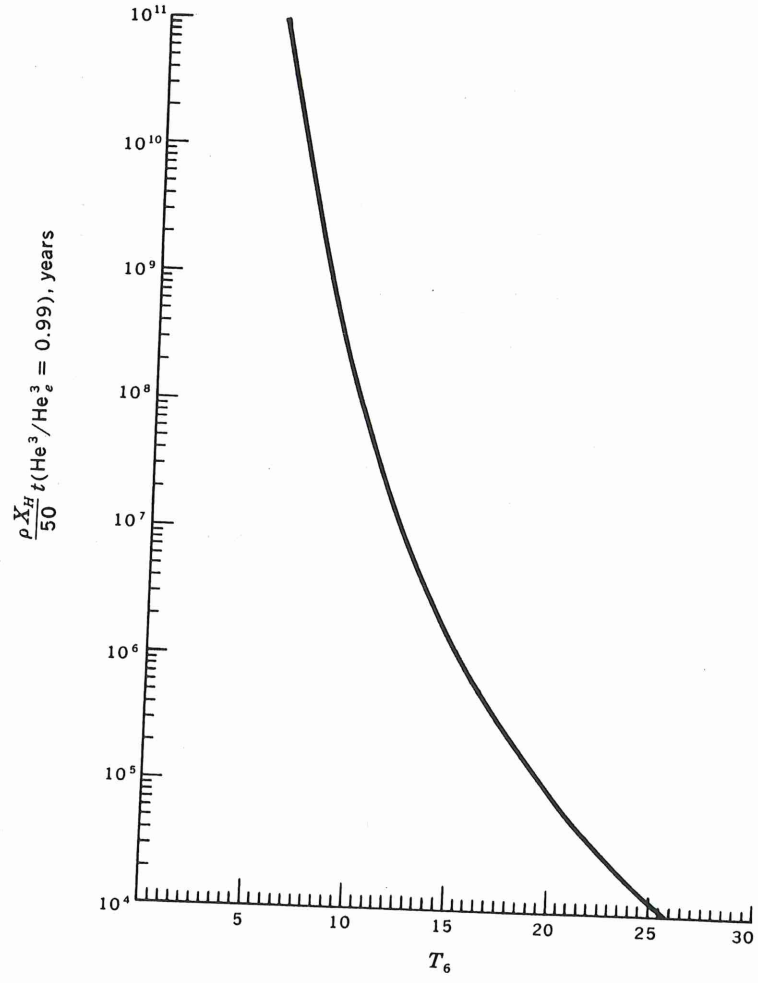

Fig. 5-6 The time required for He^3 to build up to 99 percent of its equilibrium abundance. Because this time exceeds 1 billion years for $T_6 < 8$, it is seldom reasonable to assume that He^3 has achieved equilibrium at such low temperatures.

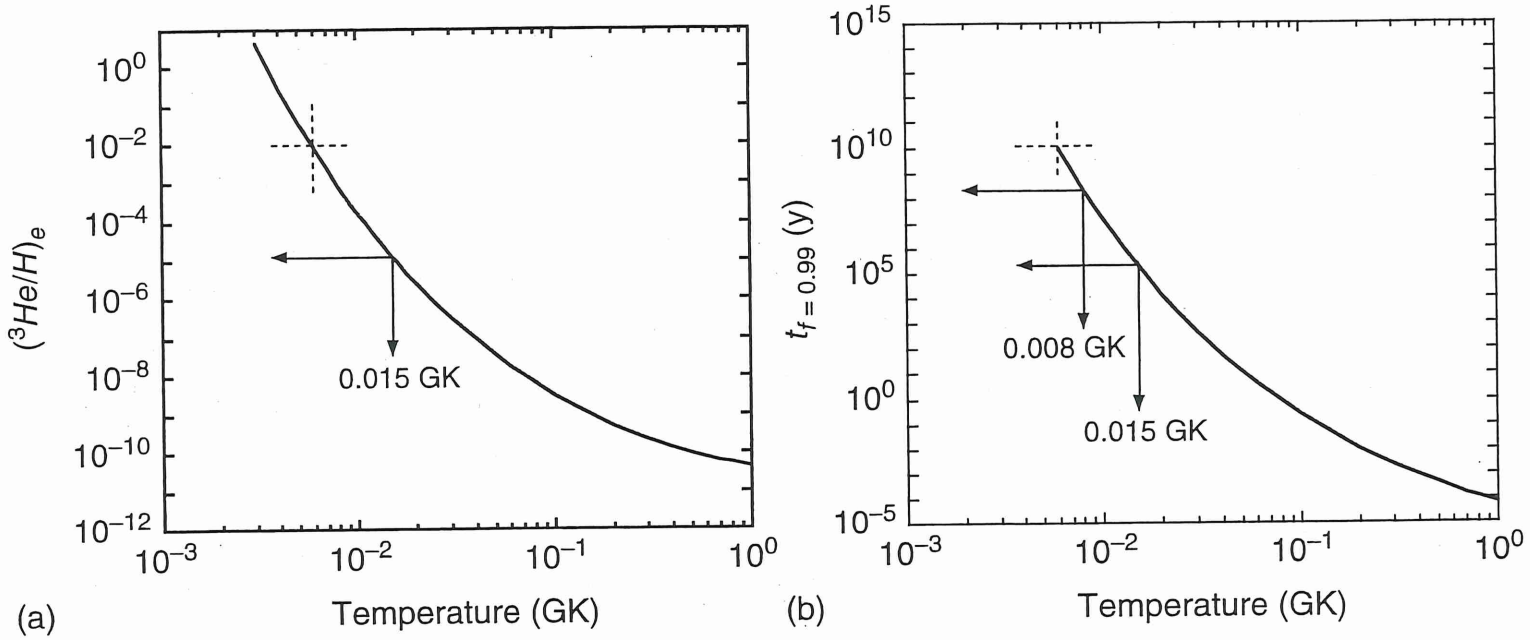

Figure 5.4 (a) Equilibrium abundance ratio $(^3He/H)_e$ versus stellar temperature. (b) Time required for ^{3}He to reach 99% of its equilibrium abundance versus temperature. The curve is calculated for the conditions $\rho = 100$ g/cm^3 and $X_H = 0.5$.

THE COLD CNO-CYCLES

→ BETA-UNSTABLE INTERMEDIARIES DECAY BEFORE p-CAPTURE

- CN proposed by BETHE 1939
  - I by von WEIZSÄCKER 1938
  - II B²FH
  - III Rolfs & Rodney 1974
  - IV ?

- C+N+O CONSERVED BUT RATIOS ALTERED
- BRANCHING POINTS when $(p,\alpha) >> (p,\gamma)$

^{15}N, ^{17}O, ^{18}O, ^{19}F

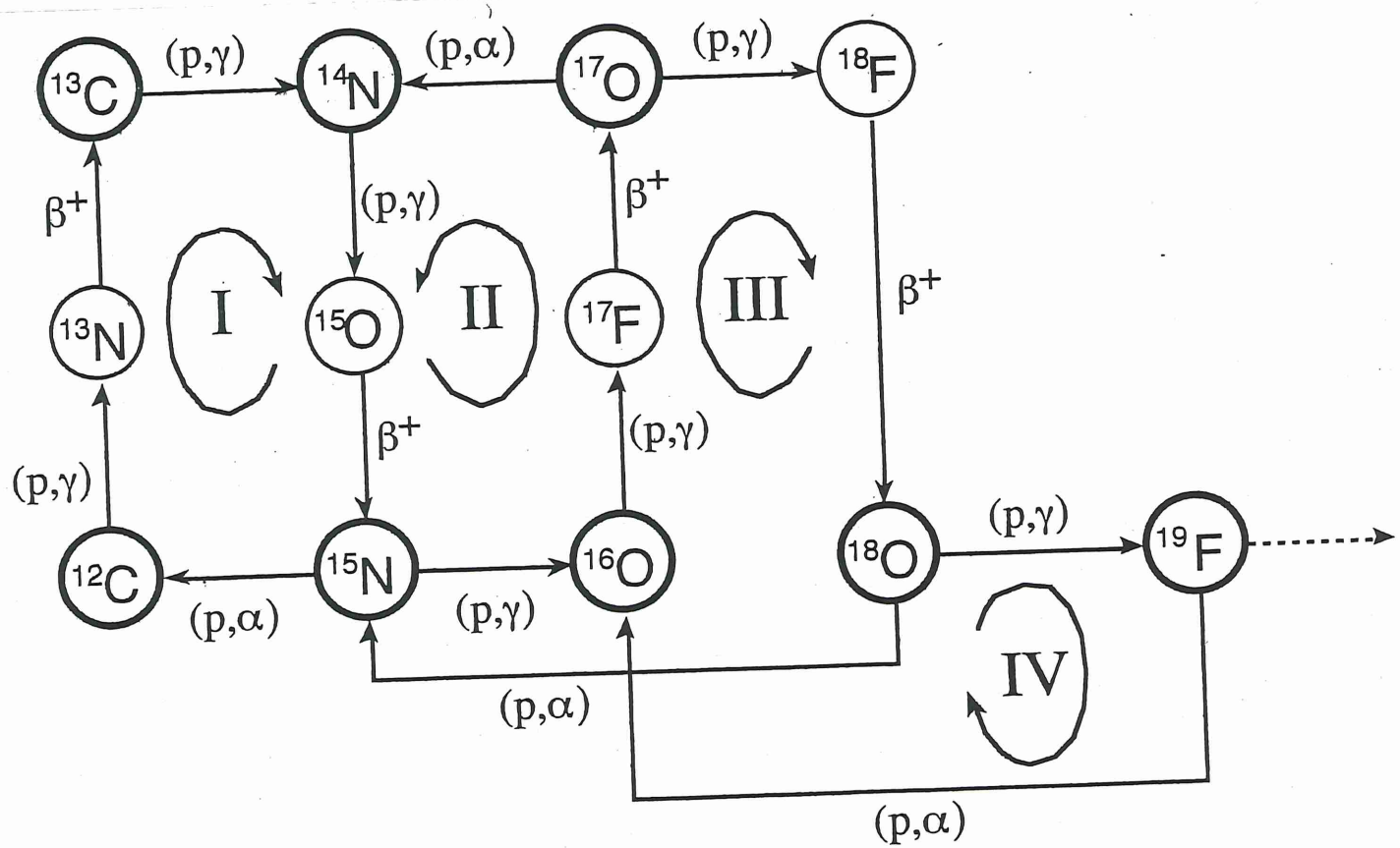

Fig. 3.2. The CNO-cycles that convert hydrogen to helium. H-burning is mainly accomplished by cycle I, often called the CN-cycle. Stable nuclides are indicated by the thicker circles. Leakage from the CNO-cycles via $^{19}F(p,\gamma)^{20}Ne$ is represented by a dashed line.

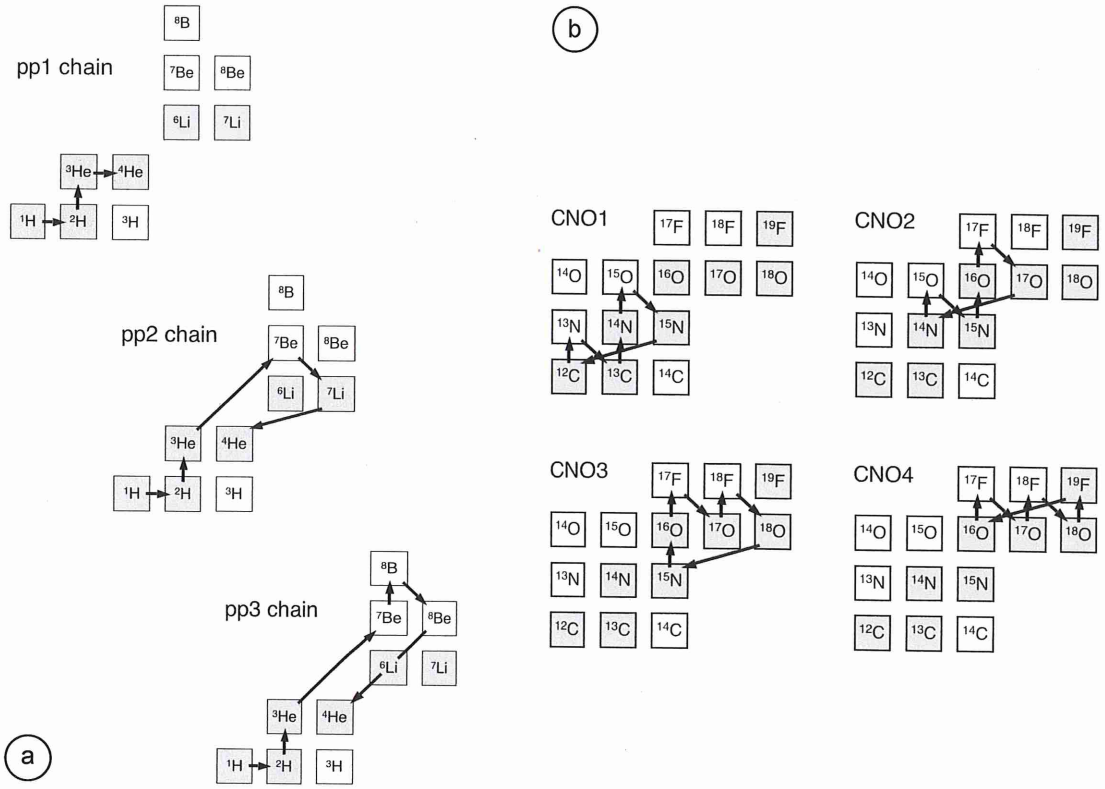

FIGURE 3. The pp chains (part a) and the CNO cycles (part b) shown schematically in the chart of the nuclides. Each arrow represents a specific interaction, connecting an initial with a final nuclide. Stable nuclides are shown as shaded squares. The proton and neutron numbers increase in the vertical and horizontal directions, respectively.

$\tau_{1/2}$ ^{13}N 9.96 min ^{15}O 122 s ^{17}F 64 s ^{18}F 110 min

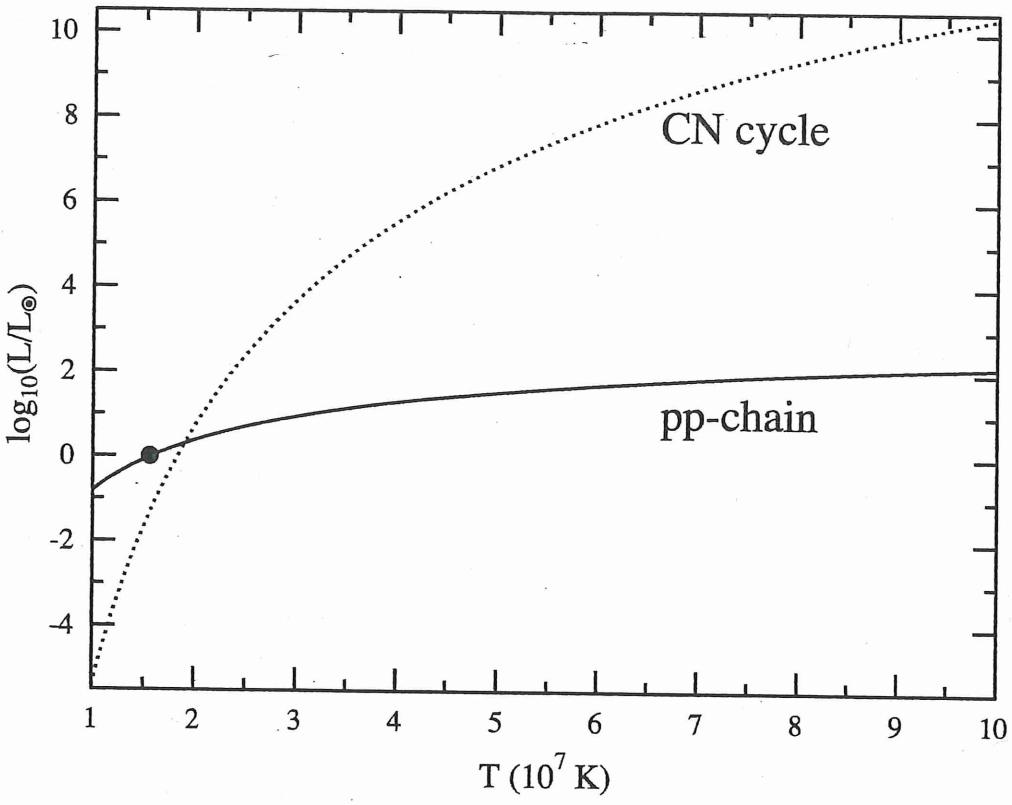

FIG. 1. The stellar energy production as a function of temperature for the pp chain and CN cycle, showing the dominance of the former at solar temperatures. Solar metallicity has been assumed. The dot denotes conditions in the solar core: The Sun is powered dominantly by the pp chain.

CNO I vs CNO II

$^{15}N(p,\alpha) \gg {}^{15}N(p,\gamma)$

T_6	$^{15}N(p,\alpha)$	$^{15}N(p,\gamma)$	RATIO
10	4.8-18	4.3-21	1120
20	7.4-12	6.5-15	1140
30	7.5-9	6.4-12	1170

~ 1000 cycles in I before a leakage to II

~ 4000 protons consumed before leakage

CNO-III introduced in 1974/5 when $^{17}O(p,\gamma)$ was shown to be more competitive with $^{17}O(p,\alpha)$

T_6	(p,γ)	(p,α)	Ratio
10	$6.7,-25$	$1.7,-24$	2.5
20	$3.8,-8$	$1.4,-17$	3.7
30	$2.2-14$	$1.4-12$	64

BUT SEE ILIADIS / Fig 5.9

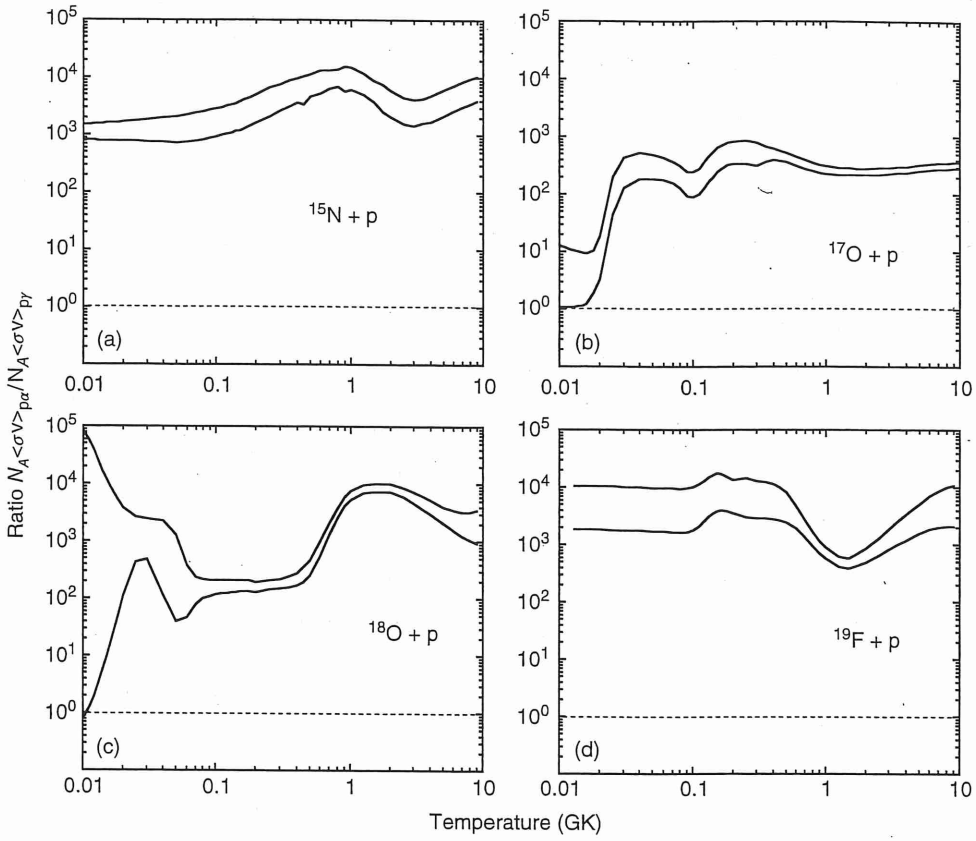

Figure 5.9 Branching ratio $B_{p\alpha/p\gamma} = N_A\langle\sigma v\rangle_{(p,\alpha)}/N_A\langle\sigma v\rangle_{(p,\gamma)}$ versus temperature for the reactions (a) $^{15}N + p$, (b) $^{17}O + p$, (c) $^{18}O + p$, and (d) $^{19}F + p$. The two solid lines in each panel represent the upper and lower boundaries of $B_{p\alpha/p\gamma}$. The area between the solid lines indicates the uncertainty in $B_{p\alpha/p\gamma}$ that is caused by unknown contributions to the (p,γ) and (p,α) reaction rates.

CNO-IV leakage to ^{20}Ne is small

T_6	$^{19}F(p,\alpha)$	(p,γ)	ratio
20	3.8-17	9.5-21	4000
30	1.3-13	3.4-17	3820
40	2.3-11	5.9-15	3920
60	1.4-8	3.8-12	3700

CNO-III loss to IV at ^{18}O

	$(p\alpha)$	(p,γ)	
20	1.4-14	1.1-17	490
30	2.6-11	2.3-14	420
40	3.1-9	5.4-12	570
60	2.9-6	2.1-8	140

CNO-I IN EQUILIBRIUM

$$\left(\frac{dn_i}{dt}\right)_{form} = \left(\frac{dn_i}{dt}\right)_{dest}$$

- ^{13}N etc. decay
- No branching at ^{15}N

TABLE 3.1
Lifetimes in the CN Cycle

	$\log \frac{\tau \rho X_H}{100}$				
T_6	^{12}C	^{13}C	^{14}N	^{15}N	α/γ
6	14.41	13.80	17.73	13.40	1050
8	11.50	10.88	14.48	10.14	1090
10	9.43	8.81	12.18	7.82	1100
20	3.91	3.30	6.06	1.63	1140
30	1.24	0.63	3.11	−1.37	1170
50	−1.65	−2.24	−0.06	−4.62	1200
70	−3.29	−3.88	−1.86	−6.50	1310
100	−4.84	−5.42	−3.54	−8.31	1540

Table Notes

a. Lifetime τ is in years and ρX_H in g cm^{-3}.

b. $\alpha/\gamma = <\sigma v>_{^{15}N(p,\alpha)} / <\sigma v>_{^{15}N(p,\gamma)}$

c. The positron emitters have mean lifetimes $\tau(^{13}N) = 870$ s or $\log \tau = -4.56$ y and $\tau(^{15}O) = 178$ s or $\log \tau = -5.25$ y.

Equilibrium, for example

$$\frac{^{12}C}{^{13}C} = \frac{\langle \sigma v \rangle_{^{13}C(p,\gamma)}}{\langle \sigma v \rangle_{^{12}C(p,\gamma)}} \; ; \quad \frac{^{14}N}{^{12}C} = ?$$

TABLE 3.2
Equilibrium Abundance Ratios in the CN-Cycle

T_6	$^{14}N/^{12}C$	$^{12}C/^{13}C$	$^{14}N/^{15}N$
6	2090	4.1	21,200
8	970	4.2	22,000
10	570	4.2	22,900
20	140	4.1	26,800
30	74	4.1	30,200
50	38	3.9	35,600
70	27	3.9	43,500
100	20	3.8	58,800

ON-cycle at equilibrium (CNO-I, I)

- <σv> uncertainties remain ?
- Equilibrium O isotopic ratios

TABLE 3.4
Equilibrium Abundances of the Oxygen Isotopes

T_6	$^{16}O/^{17}O$	$^{16}O/^{18}O$	$^{16}O/^{14}N$
6	5.1	4.6,4	1.0
8	4.1	8.6,4	0.48
10	3.5	5.6,4	0.28
20	4.8	1.8,4	0.068
30	220	2.6,5	0.033
50	920	4.4,5	0.016
70	470	3.4,6	0.0098
100	110	1.5,7	0.0057

= Exercise for the student !

NUCLEOSYNTHESIS NOTES

- $^{12}C/^{13}C \sim 4$, even if few protons consumed
- $^{14}N/^{15}N \gg (^{14}N/^{15}N)_\odot$ and ISM

  $\therefore$ ^{15}N NOT A PRODUCT OF COLD CN-CYCLING H-BURNING

  BUT COMES from HOT CNO CYCLE, Probably in NOVAE
- CN-cycles convert C to N but C/N ~ 4 IN main seq. stars.

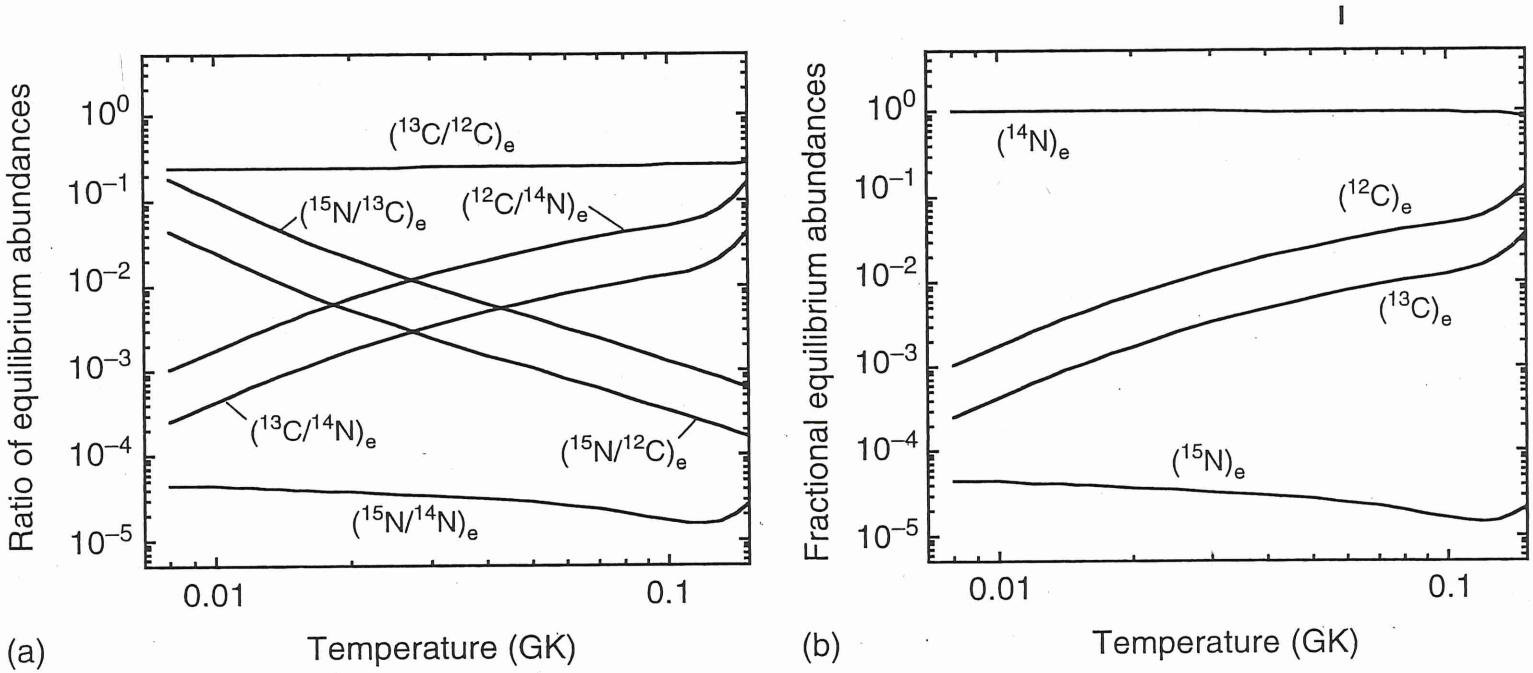

Figure 5.11 (a) Abundance ratios and (b) fractional abundances versus temperature. The curves are calculated by assuming steady-state operation of a closed CNO1 cycle.

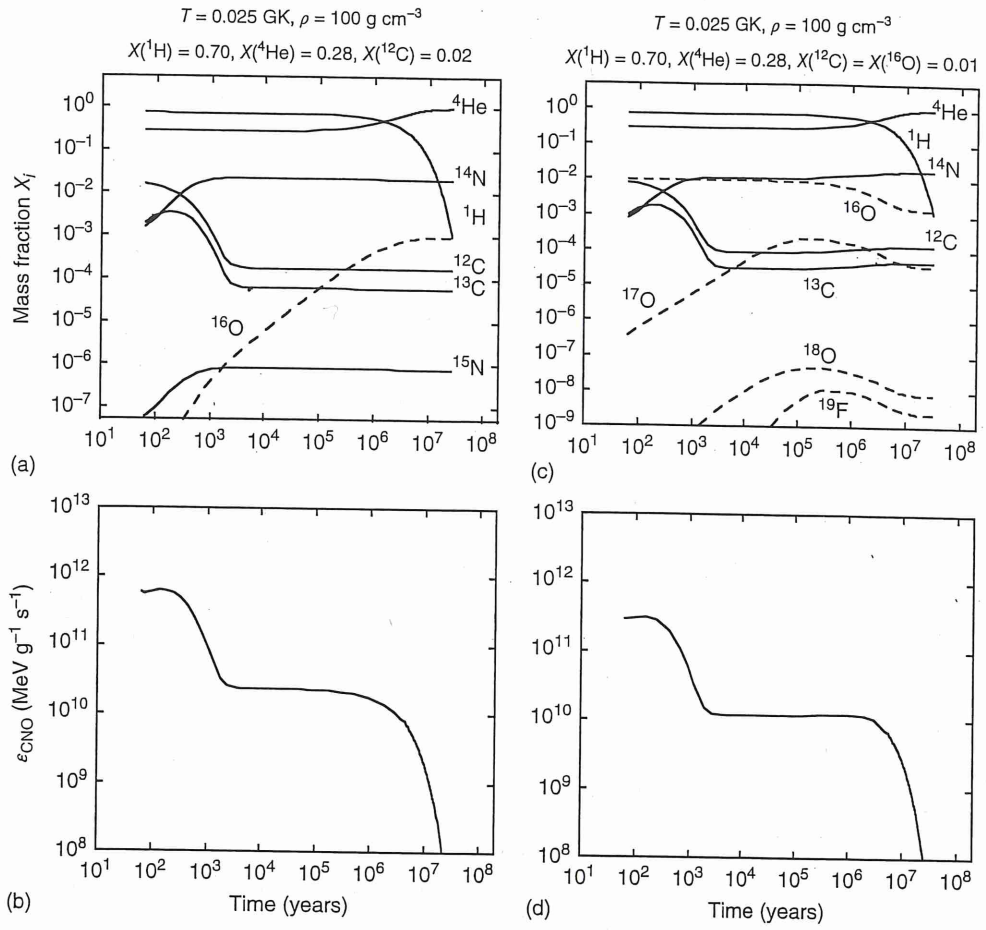

Figure 5.13 Time evolution of abundances and nuclear energy generation rate for two different compositions: (a), (b) $X^0_H = 0.70$, $X^0_{^4He} = 0.28$, $X^0_{^{12}C} = 0.02$, and (c), (d) $X^0_H = 0.70$, $X^0_{^4He} = 0.28$, $X^0_{^{12}C} = X^0_{^{16}O} = 0.01$. For the temperature and density, constant values of $T = 25$ MK and $\rho = 100$ g/cm^3 are assumed in both cases. All curves shown are obtained by solving the reaction network numerically. The calculations are terminated when the hydrogen mass fraction falls below $X_H = 0.001$.

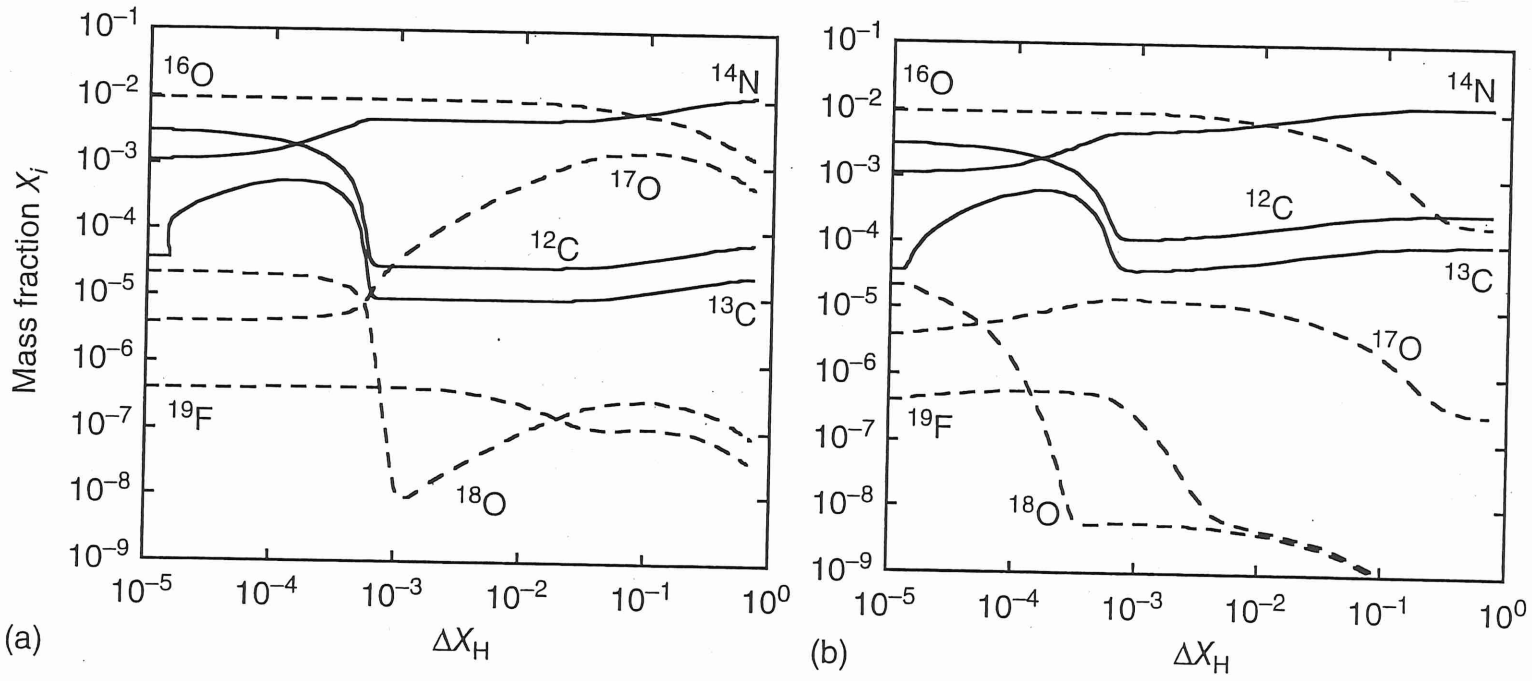

Figure 5.14 Abundance evolutions versus the amount of hydrogen consumed for two different constant temperatures: (a) $T = 20$ MK, and (b) $T = 55$ MK. The density ($\rho = 100$ g/cm^3) and the initial composition (solar) is the same for both cases. All curves shown are obtained by solving the reaction network numerically. The calculations are terminated when the hydrogen mass fraction falls below $X_H = 0.001$.

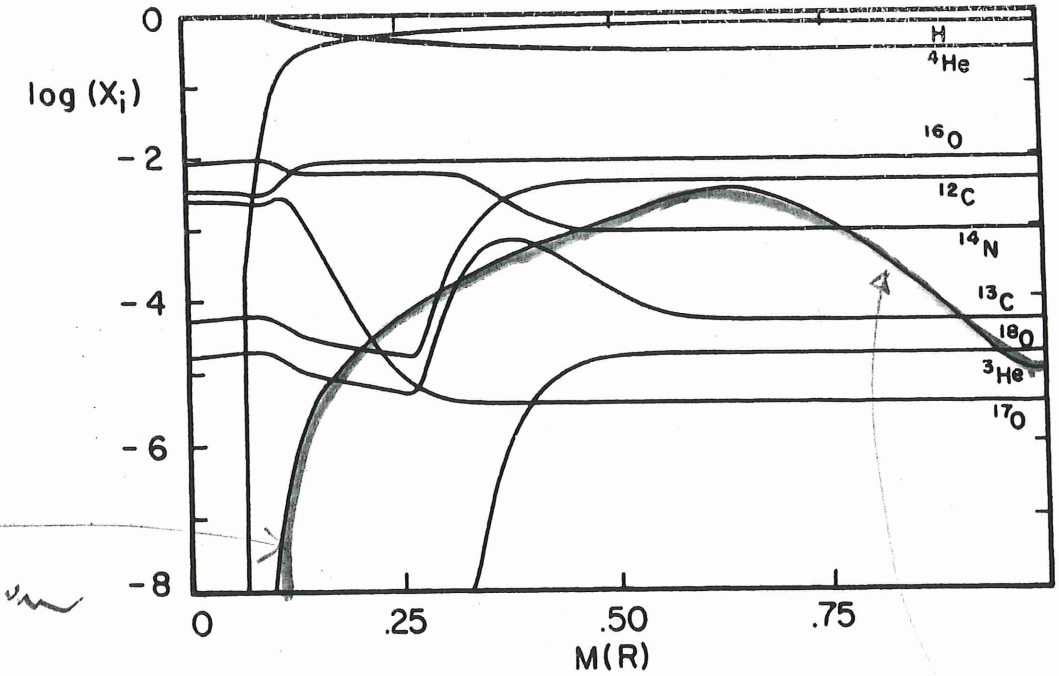

FIG. 1.—Composition of a 1 $M_\odot$ star near the end of its main-sequence evolution

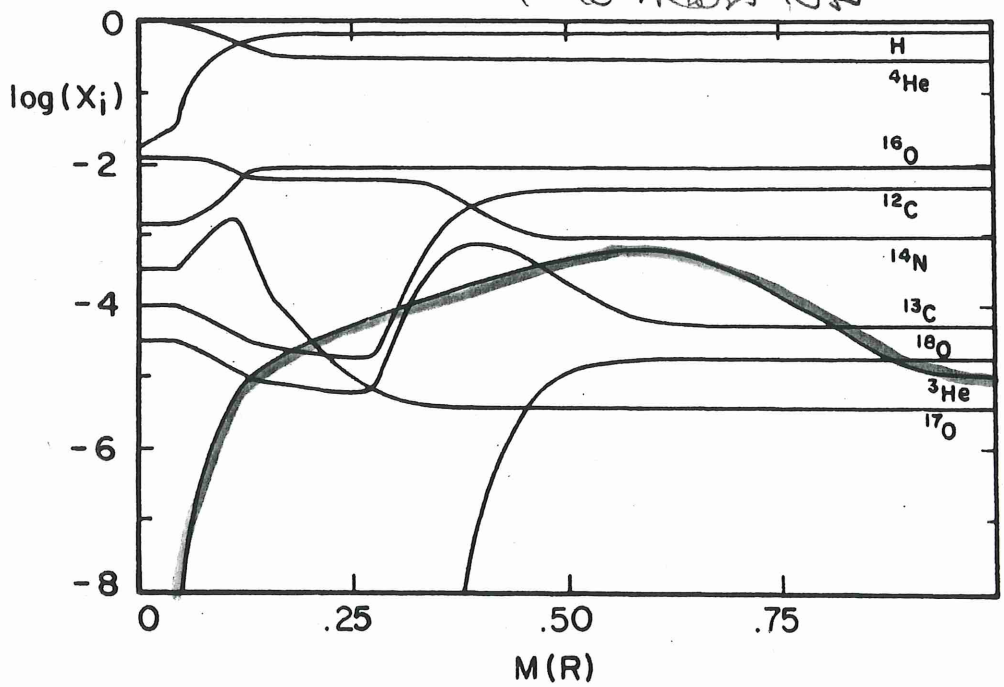

FIG. 2.—Composition of a 2 $M_\odot$ star near the end of its main-sequence evolution